Optimization of damage repair with piezoelectric actuators using the Taguchi method

Abdul Aabid
Department of Engineering Management, College of Engineering, Prince Sultan University, PO BOX 66833, Riyadh 11586, Saudi Arabia
aaabid@psu.edu.sa

Meftah Hrairi*, Jaffar Syed Mohamed Ali
Department of Mechanical and Aerospace Engineering, Faculty of Engineering, International Islamic University Malaysia, P.O. Box 10, 50725 Kuala Lumpur, Malaysia
meftah@iium.edu.my, jaffar@iium.edu.my

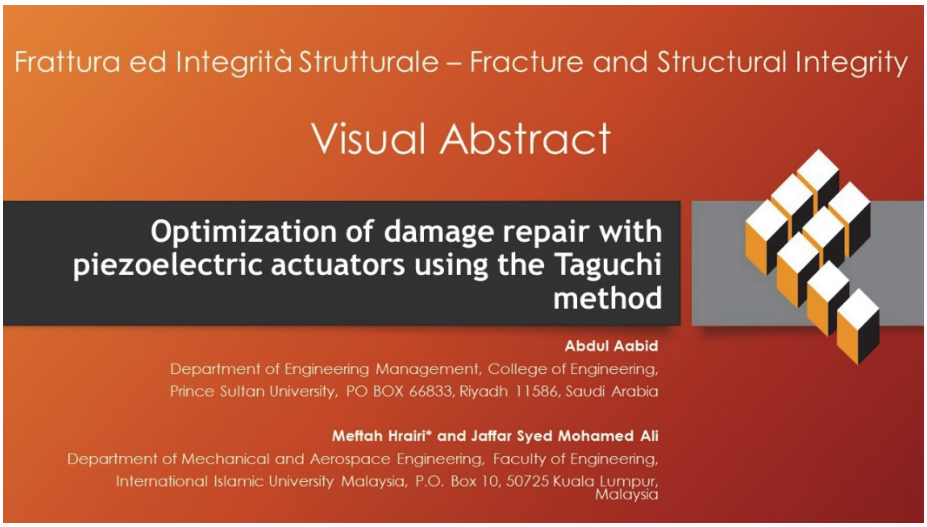

Citation: Aabid, A., Hrairi, M., Mohambed Ali, J. S., Optimization of damage repair with piezoelectric actuators using the Taguchi method, Frattura ed Integrità Strutturale, 67 (2024) 137-152.

Received: 20.08.2023
Accepted: 09.11.2023
Online first: 19.11.2023
Published: 01.01.2024

KEYWORDS. Active control, Cracks, PZT material, Finite element method, Optimization, Structures.

INTRODUCTION

Monitoring/Repairing of existing structures as a foundation for the evaluation of structural safety is becoming extremely important due to the rising number of aging structures. One of the key goals of monitoring the health and repairing of structures results in guarantee structural integrity [1], [2]. Engineering is using smart materials more frequently, which improves their capacity to fix defects and cracks in the structures and can monitor the health of

structure. PZT material utilization for active structural repair has picked up popularity. A research-focused strategy to reduce stress singularity is supported by the generation of specific forces using PZT actuator layers. This strategic technique successfully prevents the degradation of rigidity caused by bend configuration discontinuities inside cracked or defective zones. The use of PZT materials highlights innovation as well as the imperative need for improved structural recovery. This trend represents an advancement in the field of material-driven repairs, demonstrating the developing interaction between cutting-edge materials research and practical engineering applications.

The application of PZT actuators for repairing cracked structures has gained substantial attention and exploration within the research community. Wang et al. [3] began searching into whether it would be possible to use PZT actuators to fix a cracked beam. Their investigation, which concentrated on a static transverse loading situation, provided insight into the potential effectiveness of this novel strategy. Using this as a foundation, Wang and Quek [4] expanded the idea to repair a column, showcasing the adaptability of PZT actuators in dealing with different structural components. Further contributions to this field include Rogers [5], who delved into the reduction of strain concentration near notches, holes, and regions with high-stress concentrations. By employing PZT actuators, they explored how controlled deformations could mitigate stress concentrations, contributing to enhanced structural durability. Wang et al. [6] took a dynamic perspective by establishing a closed-loop feedback control system. Their study concentrated on repairing under dynamic stress conditions utilizing a notched beam coupled with PZT actuators. Their study illuminated the potential of PZT actuators to actively manage dynamic crack behaviour, a crucial consideration for real-world applications. Shah et al. [7] examined the effects of PZT actuators near holes in plates, aiming to reduce stress concentration factors (SCF). This investigation showcased the actuator's ability to influence stress distributions around stress concentration regions, thereby improving structural resilience. Alaimo et al. [8], [9] developed a boundary element technique-based repair approach that uses PZT actuators. Their study demonstrated the adaptability of PZT-based solutions within various analytic frameworks and provided a different path for crack repair.

Platz et al. [10] explored the suppression of crack propagation in homogeneous thin aluminium plates using PZT actuators. The investigation not only highlighted the ability of PZT actuators to modify crack behaviour but also emphasized their potential for lightweight structural applications. The study of SIF in plates combined with PZT actuators was significantly assisted by Abuzaid et al. [11]–[13]. They conducted parametric tests, evaluated the impacts of actuator voltage, and included setups with both centre and edge cracks. The study offered approaches to enhance the structural restoration process by delivering insightful information about the dynamic interaction between actuators and cracks [14], [15]. Aabid et al. [16] introduced a novel modelling approach involving an aluminium plate with a hole, where PZT actuators and composite patches were employed for repair. This multi-faceted configuration emphasized the evolving complexity and sophistication of PZT-driven repair methodologies.

Recently, a study has shown that the analysis of damage control in a thin cracked plate has been done by machine learning and the FE approach [17]. The authors focused on reducing human efforts and optimising the best possible solution for reducing crack damage propagation by optimizing the SIF. Very little work can be seen in the repair of cracked plates which can be explained in the literature [18] but the PZT techniques can be found in vibration control, noise control and health monitoring [19], and energy harvesting [20]. The collection of work captures the changing environment of using PZT actuators to repair damaged structures. These investigations highlight the wide range of possibilities for PZT-based solutions, from varying loading situations to dynamic responses and complex geometries. The investigation carried out by experts in this field highlights the ongoing efforts to improve structural rehabilitation methods and highlights the prospective trajectory of PZT actuators in solving practical engineering problems.

The design of experiments (DOE) method has been widely used in industrial applications to discover the most suitable factors for a manufacturing process that includes planning and conducting the experiments [21], [22]. These factors, with the influence of the designer's control and its variation over two or more levels in an efficient manner, are further evaluated by experiments executed based on the orthogonal array to illustrate the effect of each potential prime factor; therefore, to get the desired objective these processes allow researchers to execute an analysis revealing the most effective process and optimizing it by adjusting these factors. For the bonded repair mechanism, the DOE was utilized for a passive repair approach in which the composite patch was used to reduce the SIF [23], [24]. Generally, a composite patch closes the crack area and acts as a shear force on the crack face which shows more influence in reducing the damage propagation and value of SIF [25]. Over the last four decades, several studies have been done on the passive control method which can be seen in the literature provided by Aabid et al. [26], [27]. Previous studies show the possibility of active and passive repair and in the recent study, the authors introduce a novel approach called the hybrid (active + passive) method to repair the damaged plate which showed a significant impact on damage control [28], [29].

However, as suggested by the available research, a more focused strategy is necessary to improve the performance of active repair. Despite being a relatively new technology, it needs more attention than bonded composite repair to maximize the

effectiveness of its active repair. Although the SIF may be greatly reduced with bonded composite repair, it lacks the active control capabilities found in bonded PZT repair. Therefore, the primary objective of this research is to improve the active repair performance using the DOE method by conducting an extensive optimization study. For this initially, parameters such as the PZT actuator, adhesive thickness, and the shear modulus of adhesive were considered and varied its level. The FE method is used to initiate the data by varying parameters and their levels. Then, the investigation was carried out by employing the DOE, which proved to be judicious and allowed the application of the utmost influencing factors affecting the value of the SIF.

Geometry and Finite Element Model

Problem Definition

PZT actuators, adhesive thicknesses, and adhesive shear modulus were investigated using the FE approach. A commercial piece of software was used to carry out the numerical simulations and computing utilizing the three-dimensional FE approach [30]. In Fig. 1, there is an illustration of a rectangular plate with a central crack, where PZT actuators are adherently affixed. The plate encompasses a crack with a dimension of 2a = 20 mm, and the gap between the crack length and the PZT actuator, represented by S, measures approximately 1 mm.

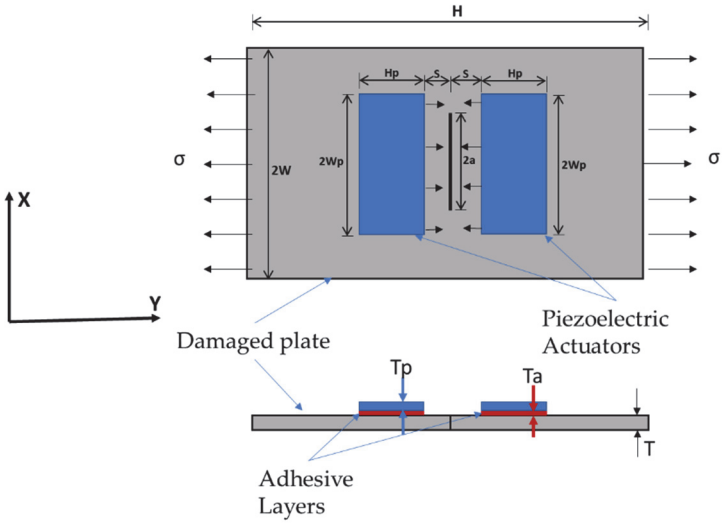

Figure 1: Geometrical model of the patched structure.

Both the aluminium plate and the adhesive are presumed to exhibit elastic properties. The stress-strain curves for the aluminium alloy 2024-T3 [31] and the Araldite 2015 adhesive [32] are visualized in Figs. 2a and 2b respectively. The plate underwent a consistent uniaxial tensile load, where the stress was maintained at σ = 1 MPa.

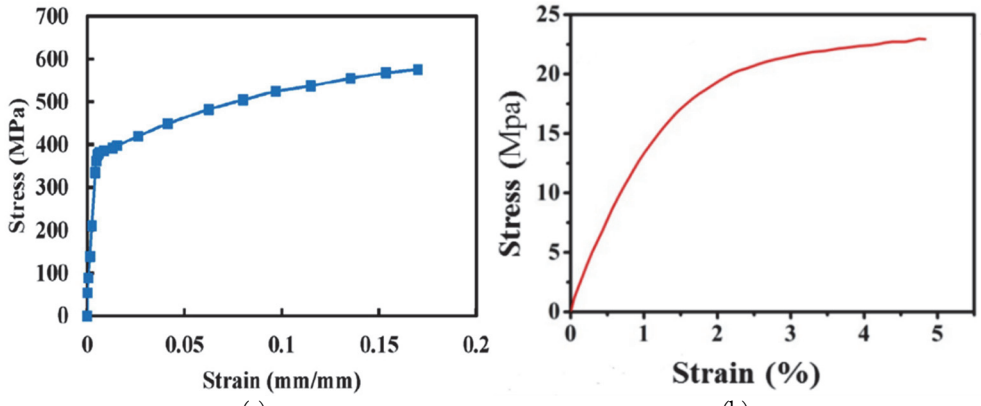

(a) (b)

Figure 2: Basic stress-strain curve. (a) Aluminium alloy 2024-T3 [31] (b) Araldite 2015 [32].

Tabs. 1 and 2 provide an overview of the geometric specifications and material characteristics of the aluminium plate, PZT actuator (PIC 151), and adhesive bond (Araldite 2015).

Parameter	Cracked Plate	PIC151 Patch	Adhesive
Hight	H=200	Hp=20	Ha=20
Width	2W=80	2Wp=40	2Wa=40
Thickness	T=1	Tp=0.3	Ta=0.03

Table 1: Dimensions of the plate, actuator, and adhesive bond.

Parameter	Cracked Plate	PIC151 Patch	Adhesive
Density	2715 kg/m^3	7800 kg/m^3	1160 kg/m^3
Poisson's Ratio	0.33		0.345
Young's Modulus	68.95 GPa		5.1 GPa
Shear Modulus			1.2 GPa
Compliance Matrix	4	$S_{11} = 15.0\times10^{-12}$m^2/N $S_{33} = 19.0\times10^{-12}$m^2/N	
Electric Permittivity Coefficient	5	$\varepsilon_{11}^{T} = 1977$ $\varepsilon_{33}^{T} = 2400$	
PZT strain coefficient	9	$d_{31} = -2.10\times10^{-10}$m/V $d_{32} = -2.10\times10^{-10}$m/V	

Table 2: Properties of the plate, actuator, and adhesive bond.

Simulation Model

Coupled-field analysis, which addresses the interplay between structural and electric fields, is included for PZT analysis. For numerical simulation, the modelling of the PZT actuators was made by coupled field SOLID226 element type which is accessible in ANSYS 18.0. SOLID226 contains 20 nodes per element with 5-DOF for each node. The modelling of the adhesive layer and aluminium plate was done by SOLID186 element type. SOLID186 has a higher order of 20 noded elements, which is suitable for a solid-structures simulation. These element types are suggested for linear elastic fracture mechanics (LEFM) problems. Fig. 3 shows the numerical mesh model of the plate with a PZT actuator. Since the model geometry and applied load are symmetric, only one-quarter of the structural model was analyzed. To model the crack front; 10 singular elements were generated.

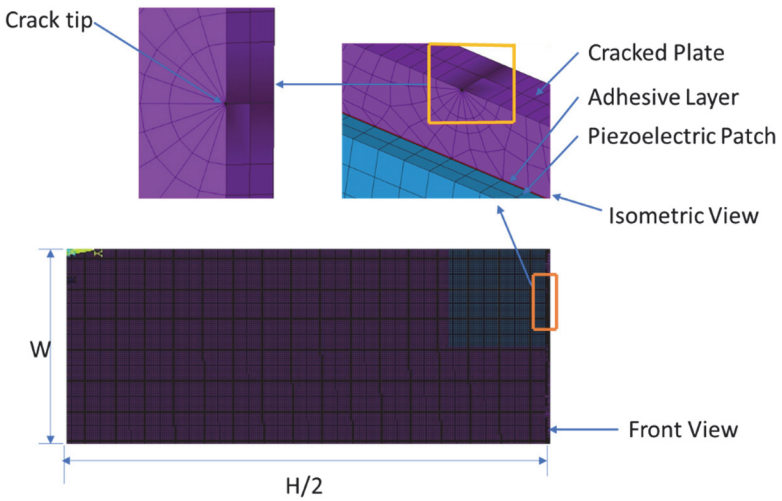

Figure 3: Numerical mesh model.

To model a PZT actuator, a coupled-field element was used; mesh elements consisted of 4999, whereas to model the aluminium plate and adhesive bond, 74,988 and 2499 solid elements were used respectively. The PZT actuator applied an electric field at the voltage of 150 in all cases of the present study to obtain the SIF results. It is important to highlight that the SIF unit utilized in this study has been standardized as MPa√m. To maintain clarity and precision, the notation "SIF" or "K" has been singularly employed, thereby circumventing the need for repeated unit representation.
The FE method consists of three subsets to model the aluminium plate, the adhesive bond, and the PZT actuator. PZT actuator analysis emanates under the coupled-field element examination category, which provides the interaction between electric and mechanical fields.

Mesh convergence study

Tab. 3 provides more information on the three distinct mesh dimensions that were chosen to evaluate the effect of mesh size on computational results. A grid-structured technique was used to mesh the adhesive bond and the PZT actuator, and the component size was matched to the appropriate mesh type. To create an unstructured mesh design, the pieces were divided for the damaged plate. A modest improvement in the accuracy of the computed SIF (K) value, with a maximum relative deviation of 14%, was seen as the mesh was refined from medium to fine dimensions, as shown in Tab. 3. But the medium-sized mesh provided sufficient resolution and accuracy while requiring just half the processing time, making it the better option for the next simulations.

Mesh Type	No. of Elements	No. of Nodes	CPU Runtime (seconds)	SIF (K)
Coarse	11832	28692	309	0.11335
Medium	33452	73633	600	0.09668
Fine	68920	133633	1522	0.09368

Table 3: Mesh convergence study.

Validation of the FE model

Tada's analytical solution [33] holds significance as a foundational approach for calculating SIF in center cracked plates. It is an essential relation in fracture mechanics, offering insights into crack propagation and structural integrity under diverse loading conditions. This solution enables engineers and researchers to assess the critical conditions of cracked structures, aiding in the design and maintenance of safe and robust engineering components. Therefore, this fracture mechanics analytical solution was used to evaluate the simulation model of the unrepaired plate initially. There is a good agreement between the findings obtained by Tada's analytical solution following Eqn. (2) and the current simulation results, as shown in Tab. 4.

$$K_I = \sigma\sqrt{\pi a}\sqrt{\frac{2b}{\pi a}tan\frac{\pi a}{2b}}\frac{0.752+2.02\left(\frac{a}{b}\right)+0.37\left(1-sin\frac{\pi a}{2b}\right)^3}{cos\frac{\pi a}{2b}} \quad (1)$$

where a denotes the length of the crack and b denotes the breadth of the cracked plate.

Condition	Theoretical [33]	Current Simulation	Relative Error
Without Repair	0.1772	0.1774	0.117%

Table 4: Validation of numerical simulation results (without repair).

The strong agreement between the two outcomes is illustrated in Fig. 4, demonstrating the correctness and reliability of the computational model as a realistic representation of the experimental work. The default model was chosen to compare the simulation results which can be seen in the work done by Abuzaid et al. [13] and it is similar to the problem defined in this work (Fig. 1). The crack length of the plates was used 2a = 20 mm and voltage varied from 25 to 100 V. The maximum relative discrepancy of roughly 10% implies that the disparities between simulation and actual outcomes are rather minimal, given the challenges associated with performing real-world trials. Despite these small differences, it is crucial to understand

that a number of variables, including conceivable human error, may have had an impact on how precisely the experimental findings were obtained while placing and aligning the strain gauge and PZT actuator on the host plate. Additionally, the experimental results may have been impacted by the little notch outside of the computational model that caused the crack. The small differences between the two sets of data might be explained by the presence or absence of these variables. Overall, the linear oscillation of the SIF (K) in response to the applied electric field retains congruence with the underlying principles, confirming the accuracy and integrity of the computational model.

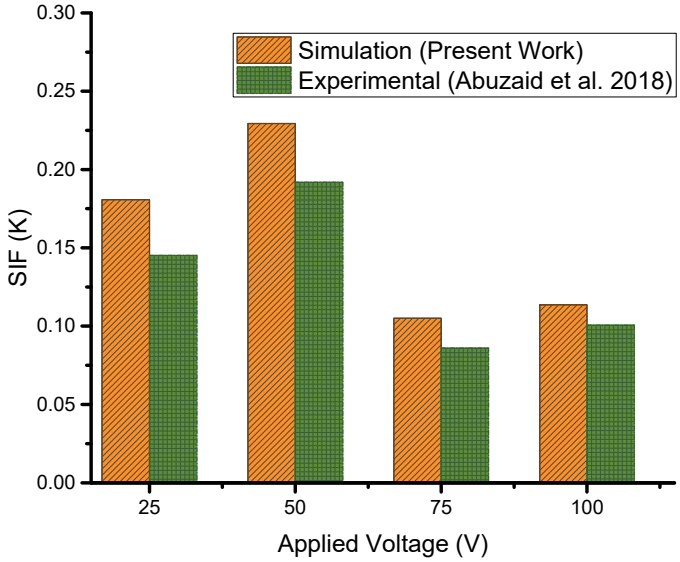

Figure 4: Validation of current FE findings using experimental data from [13] (with repair).

OPTIMIZATION METHOD

Yala et al. [34], [35] and Fekih [36] used the optimization method via DOE to optimize repair in aircraft structures using bonded composite patches. In this work, a center-cracked rectangular aluminium 2024-T3 plate was considered and was integrated with the PZT actuator under uniform uniaxial tensile load as shown in Fig. 1. A perfectly bonded PZT actuator prevented the propagation of the crack close to the high-stress area on one side of the aluminium plate from inducing stresses through an electric field for repair of the plate. The process of the optimization can be seen in Fig. 5.

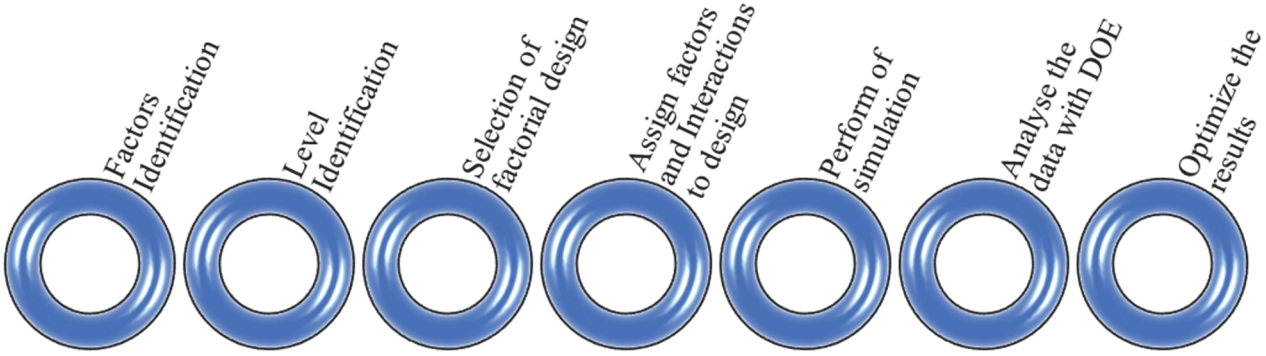

Figure 5: Process of optimization study.

For the parameter optimization of a given problem with a known function of an objective, the most suitable method is the DOE which can quickly optimize the different factors to obtain an optimum result. As we aim to reduce the SIF, that is a function which has numerous variables whose values can probably be controlled. Therefore, the DOE method is suitable for hire. For this specific case, three factors were considered that affect the value of SIF (K): the actuator (Tac) and the adhesive (Tad) thickness, and the shear modulus of the adhesive (G). The goal was to find the optimal values of these factors that help in the reduction of SIF. Each value of factors is called levels (treatments) as shown in Tab. 5.

Factors	Levels		
	1	2	3
Actuator Thickness (mm)	0.5	0.75	1.0
Adhesive Shear Modulus (MPa)	882	954	1022
Adhesive Thickness (mm)	0.025	0.03	0.035

Table 5: Selected parameter variables

Taguchi's L_9 orthogonal array

Taguchi design (robust parameter design) suggested highly fractionated factorial designs and other orthogonal arrays along with some novel statistical methods to solve these types of problems [22]. If resources like cost and time are available, opting for an L_9 orthogonal array is advisable. This choice is advantageous because it allows for comprehensive testing of multiple parameters at various levels, including all three levels of other variables. On the other hand, if conducting a full factorial analysis entails significant costs and time investment, and problem-solving the accuracy of outcomes is not of utmost importance, then the application of the orthogonal Taguchi array method is recommended. The orthogonal array is typically used in industrial applications to investigate the impact of various control parameters. Additionally, the columns for the independent variables are orthogonal to one another in this form of study. To outline an orthogonal array, it's essential to establish distinct levels and constituents which can be seen in Tab. 6.

Runs	Coded Values			Response Output
	A	B	C	
S1	X1	X1	X1	Y1
S2	X1	X2	X2	Y2
S3	X1	X3	X3	Y3
S4	X2	X1	X2	Y4
S5	X2	X2	X3	Y5
S6	X2	X3	X1	Y6
S7	X3	X1	X3	Y7
S8	X3	X2	X1	Y8
S9	X3	X3	X2	Y9

Table 6: Taguchi's L_9 orthogonal array.

FINITE ELEMENT RESULTS BASED ON THE TAGUCHI TABLE

The initial phase involved simulations utilizing Taguchi's orthogonal array, with a total of 9 simulations conducted on the repaired plate, maintaining a constant voltage of 150 V. This voltage choice aligns with previous findings by Abuzaid et al. [13], substantiating that a maximum voltage up to 150 V remains feasible and adaptable within aircraft maintenance. The study suggests that raising the voltage correlates with a reduced SIF (K), contributing to enhanced structural integrity. However, limitations in aircraft systems restrict voltage increase. As per existing research, the optimal selection revolves around the 150 V threshold, substantiating its suitability within the aircraft domain.

From the Taguchi method, the computation of degrees of freedom (DOF) was conducted for three parameters within each of the three sets, encompassing multiple instances of level 1. A three-level L_9 orthogonal array comprising nine experimental trials was chosen. The overall DOF for the experiment amount to 8, calculated as 9 - 1. Total 9-DOF is the most suitable orthogonal array for simulation also known as L_9 array, and these values are selected in ascending order. Hence, the Taguchi orthogonal array is illustrated in Tab. 7. All the value of SIF (K) has been computed for the repaired plate whereas the value of the unrepaired plate is 0.1771 MPa$\sqrt{m}$. Based on the results obtained for an orthogonal array the higher reduction of SIF was found at approximately 0.113663 MPa$\sqrt{m}$ which is approximately 36% of the reduction in repaired bonded PZT actuator effect. The DOE technique is the primary emphasis of the current work; hence the simulation is limited to the Taguchi design with an L_9 orthogonal array. This data was then utilized to optimize the SIF (K) for certain values and levels which can be seen in the next section of this paper.

Based on the results shown in Tab. 7, careful optimization work was planned. This undertaking encompassed a range of influential techniques such as analysis of variation, response surface analysis, main effect plot, interaction plot, contour plots, coefficients table, and response optimization table. These methodologies, collectively employed, constitute a comprehensive analytical framework. The central thrust of this comprehensive analysis lies in the comparative examination of simulation and optimization outcomes.

By comparing simulation and optimization results, this comprehensive investigation offers a profound and multifaceted exploration of the field of cracked repair through the application of PZT actuators. The primary objective is to harness the capabilities of optimization techniques, thereby accentuating the understanding of how PZT-based repairs can be maximally enhanced. This exploration considers diverse facets of the repair process, ranging from individual parameters to their intricate interplays, with the overarching goal of achieving optimal repair efficiency.

Through the strategic implementation of these optimization methodologies, this study not only underscores the potential of PZT actuators for structural repair but also reinforces the significance of adopting systematic optimization approaches. Ultimately, this in-depth analysis serves as a pivotal stepping stone towards a more refined and effective utilization of PZT actuators in the realm of cracked repair, facilitating robust engineering solutions in the pursuit of enhanced structural integrity.

Simulation Runs	Input Parameters			Response – SIF (K)
	Tac	G	Tad	
1	0.5	882	0.025	0.113663
2	0.5	954	0.03	0.114051
3	0.5	1022	0.035	0.114397
4	0.75	882	0.03	0.119970
5	0.75	954	0.035	0.120351
6	0.75	1022	0.025	0.118617
7	1.0	882	0.035	0.124878
8	1.0	954	0.025	0.122862
9	1.0	1022	0.03	0.123363

Table 7: Orthogonal array (OA) L_9 with control factors runs.

OPTIMIZATION OF BONDED PIEZOELECTRIC ACTUATOR REPAIR

Tab. 6 illustrates the orthogonal array matrix of the premeditated optimization method. It comprises a Taguchi design that has all possible amalgamations accomplished by considering all three parameters; each parameter has three levels (treatments).

Before proceeding to other optimization methods, the main effects plot for SIF with factors (Tac, G, and Tad) is shown in Fig. 6. It has been detected that SIF increases highly with an increase in the thickness of the PZT actuator since we aim to reduce the SIF, this is because of the formation of the lower electric field from the thicker actuator at the crack length. However, SIF decreases slightly with the increase of adhesive shear modulus. When the thickness of the adhesive is small, it is more useful to reduce SIF due to the shear stress that increases due to the adhesive bond.

The application of DOE commonly involves assessing the average outcome of a single or repetitive trial through an ANOVA analysis. ANOVA serves as a pivotal method to compare different levels in DOE [21]. In the current study's optimization-focused environment, we used ANOVA analysis to undertake a thorough investigation of the orthogonal array. By revealing the effect of individual components and the associated error as well as any potential interactions between these factors, the ANOVA Tab. 8 serves a key role. The ANOVA table for reducing SIF in a plate, shown in Tab. 8, was taken from Minitab 18 and Design Expert 13 software in an optimization effort [37]. This was interesting to find out that the actuator thickness had little effect, whereas the shear modulus and adhesive thickness were of considerably smaller importance. The careful implementation of an 8-DOF (9 – 1 = 8 total) structure incorporating the three components and four interactions may be credited with this result. As a result, this thorough analysis effectively accounted for most of the variability, making the following results irrelevant. To overcome this challenge, an ingenious approach was employed: the effects of the non-significant factors and interactions were consolidated. The interactions DOF and corresponding sums of

squares (SS) merged due to the interactions' very small discrepancies. The construction of an "error" factor resulted from the later removal of this combination of pooled numbers from their allocated placements in Tab. 8 [38].

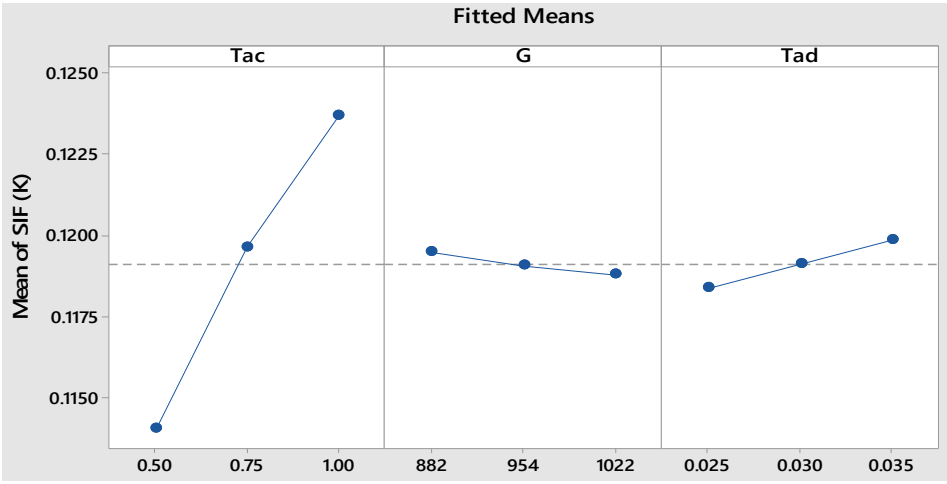

Figure 6: Main effect plots for means.

As indicated in Tab. 8, among the single-factor interactions, the thickness of the actuator emerges as the most influential parameter, with a notable F-value of 148.87. This prominence can be attributed to its ability to induce compressive effects on the crack region. Generally, higher voltages applied to PZT actuators lead to greater reductions in SIF, offering insight into its effectiveness. The examination of other parameters reveals that the adhesive thickness holds significance when it's relatively thinner, while the shear modulus of the adhesive becomes more impactful when it is higher. Turning to the realm of two-way interactions, a notable F-value of 1.64 is observed for combinations involving higher adhesive shear modulus and thickness. This signifies the combined influence of adhesive shear modulus and thickness in bonding the plate with the actuator. This phenomenon can be comprehended by considering that the utilization of all three factors and four interactions utilizes the available 8-DOF completely, leaving no room for further error assessment. To address this limitation, an effective strategy involves consolidating the effects of non-significant factors and interactions. Within this context, the interactions exhibit minor disparities, leading to the grouping of their DOF and the respective SS.

Source	DOF	SS	MS	F-Value	P-Value
Tac	1	0.000049	0.000049	148.87	0.007
G	1	0.000001	0.000001	2.26	0.272
Tad	1	0.000002	0.000002	7.09	0.117
Tac*G	1	0.000000	0.000000	0.64	0.507
Tac*Tad	1	0.000000	0.000000	0.46	0.567
G*Tad	1	0.000001	0.000001	1.64	0.329
Error	2	0.000001	0.000000		
Total	8	0.000145			

Table 8: Analysis of variance (ANOVA).

Overall, the findings from Tab. 8 highlight the crucial importance of actuator thickness in single-factor interactions as well as the complex interplay between adhesive properties in two-way interactions. The analysis is made stronger and more accurate by carefully examining the DOF and grouping specific features thereafter. In summary, the utilization of ANOVA and orthogonal array analysis in our optimization study unveils insights into the relative significance of various factors and their interactions. This approach, accompanied by strategic consolidation and error management, contributes to the precision and effectiveness of our optimization efforts.

Tab. 9 illustrates the factor coefficients and their interactions. It was observed that the factor which influenced the most was the thickness of the PZT actuator (0.004473) then it related closely with the thickness of the adhesive (0.000976). The factor coefficient of adhesive shear modulus was (-0.000541) far distant from these values. Then, two-way interactions

showed a decrease in the order of the thickness of the PZT actuator/adhesive shear modulus (0.000441), the thickness of PZT actuator/thickness of adhesive (-0.000367) and finally the adhesive shear modulus/thickness of adhesive (-0.000703). The coefficients sign was not considered because the "weight" of the coefficients only mattered. Fig. 7 supported these results; the plot of the SIF standardized effect was thus suitable for screening DOE. The PZT actuator effects had the most extensive range, while others were limited to the smallest range. It was noticed that the standardized effects were twice the coefficients and changes occurred in the response when the level of factors varied from higher to the average.

SIF (K)	Coef	SE Coef	T-Value	P-Value	VIF
Constant	0.119133	0.000192	619.76	0.000	
Tac	0.004473	0.000367	12.20	0.007	2.43
G	-0.000541	0.000360	-1.50	0.272	2.34
Tad	0.000976	0.000367	2.66	0.117	2.43
Tac*G	0.000441	0.000550	0.80	0.507	3.64
Tac*Tad	-0.000367	0.000540	-0.68	0.567	3.51
G*Tad	-0.000703	0.000550	-1.28	0.329	3.64

Table 9: Coefficient list.

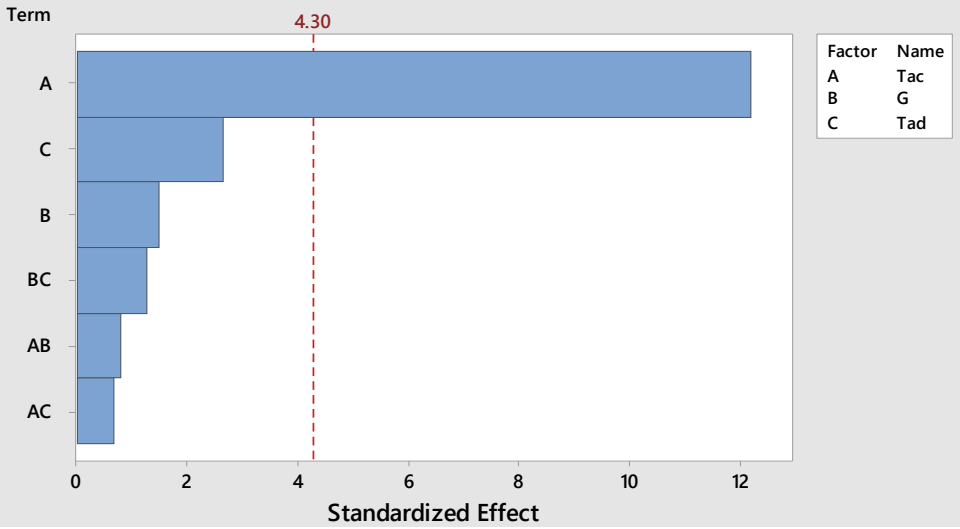

Figure 7: Effect of SIF.

Interaction plots were frequently used to predict interactions throughout the optimization method. Fig. 8 shows the interaction matrix plot for SIF; the graphs corresponding to these three levels are distant from each other except for the thickness of the PZT actuator and thickness of the PZT actuator/thickness of the adhesive. For the case of the thickness of adhesive/adhesive shear modulus and only adhesive shear modulus, the value of SIF increased/decreased; therefore, the interaction for these combinations was enabled. Moreover, the interaction was also enabled for the case of the thickness of the PZT actuator/thickness of adhesive with continuous increase of SIF with an increase of parameters thickness. Then, for the thickness of the PZT actuator, the SIF is increasing with increasing thickness. It means that the PZT electrode with the applied voltage transferred less compressive load towards the crack when the PZT thickness was higher, and when the PZT thickness was lower, the voltage effect was greater. Finally, for the case of adhesive shear modulus/thickness of the PZT actuator and thickness of the adhesive/thickness of the PZT actuator, the interaction was not visible, and the values of SIF were almost constant.

This study proved that when the thickness of the PZT actuator is high, it will result in higher SIF. Therefore, the higher thickness of the PZT actuator is not recommended to reduce SIF since the applied voltage of the actuator is 150 V. Furthermore, adhesive shear modulus gives a reduction in SIF when it increases because of an increase in shear stress. In two-way interactions, the thickness of the PZT actuator/thickness of the adhesive is the most effective method for the reduction of SIF, when it is at the lower level and similar only to the thickness of the PZT actuator. From all the interactions, the lower value of adhesive thickness and actuator thickness as well as the higher value of adhesive shear modulus is more

useful to reduce the SIF. Moreover, all terms which are displayed in the interaction plot are not in the model, and it was generated from the study of optimization through the DOE method in Minitab software.
To see all observations of SIF in the proposed design, the term polynomial expression model has been used via screening design, which is illustrated in Eqn. (2) and the obtained SIF in Tab. 10. The value of SIF which was obtained from numerical simulation and the model fit was almost closer. It indicates that the obtained numerical simulation results based on Taguchi's design almost fit the approximate solutions for the designed combination of all parameters.

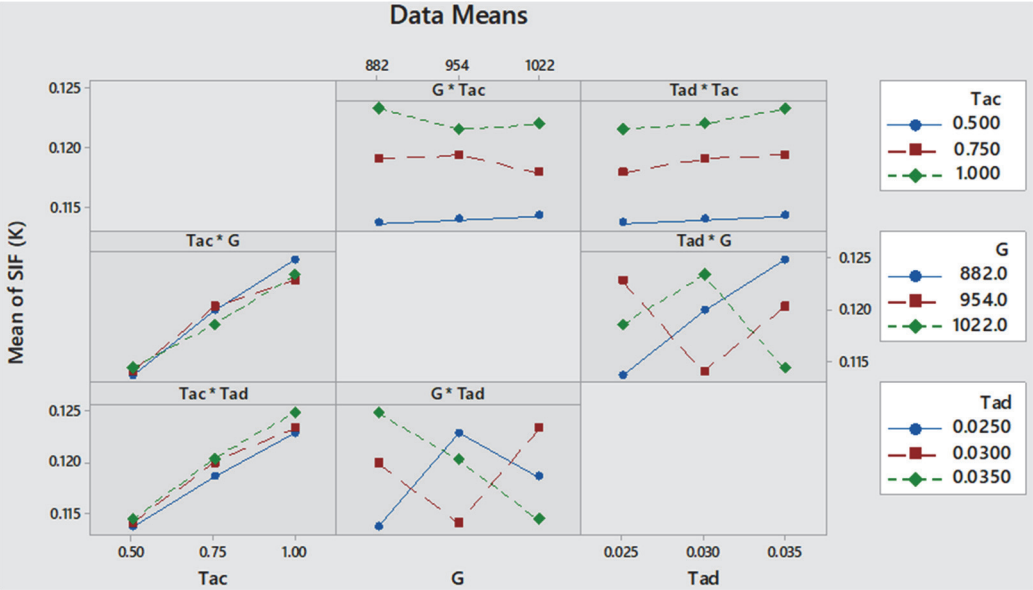

Figure 8: Parameter interactions.

To express more about this study, the results are plotted in Fig. 9. The simulation begins with the lowest value to the highest amount of SIF. The SIF increases when increasing the runs, but at observations 6 and 8 the value is less compared to the previous terms. It means that in these observations the parameters are effective compared to the previous one. The relative error between these two results is the least, as shown in Tab. 10. The substantial forecasted R^2 value of 99.15% indicates that the model's predictive capabilities are almost as proficient as its ability to match the existing sample data. The regression equation is expressed as follows.
Regression Equation,

$$SIF = 0.10499 + 0.019328\ Tac - 0.000005\ G + 0.1495\ Tad \quad (2)$$

Simulation Runs	Tac	Gad	Tad	Model fits SIF(K)	FEA SIF (K)	Percentage Error
1	0.5	882	0.025	0.113982	0.11366	0.27943
2	0.5	954	0.03	0.114369	0.11405	0.27804
3	0.5	1022	0.035	0.114777	0.1144	0.33064
4	0.75	882	0.03	0.119561	0.11997	-0.34208
5	0.75	954	0.035	0.119949	0.12035	-0.33556
6	0.75	1022	0.025	0.118114	0.11862	-0.42628
7	1	882	0.035	0.125141	0.12488	0.20976
8	1	954	0.025	0.123286	0.12286	0.34351
9	1	1022	0.03	0.123693	0.12336	0.26678

Table 10: Model fits and numerical SIF comparison.

The variation of the shear modulus of adhesive is less noticeable because it was observed that it remains approximately constant in some arrangements. The results obtained are quite approximate when compared to the results found by changing

parameters of considered interactions thus showing the novelty of this work. Once the parameter study is achieved, optimization is performed; the primary objective of this work can be attained using the contour plots shown in Fig. 10. For minimizing SIF, the lower level of PZT actuator thickness and levels 1 and 2 for adhesive thickness were selected, concerning the adhesive shear modulus, the minimum value of SIF was obtained at higher levels.

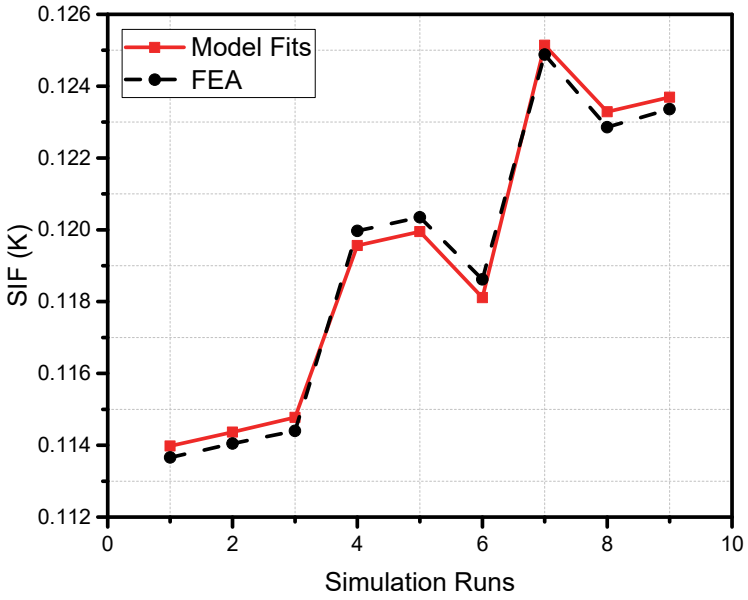

Figure 9: Comparison of simulation and modal prediction.

The contour shows the three different sets of variables. Keeping one value constant with the other two values will show the combination of parameters and the results of SIF. The adhesive and actuator thickness can be seen in Fig. 10(a) and the variation in SIF (K) was found to be very low when these two-variable values were in the initial stage and high at the final stage. The actuator thickness vs adhesive thickness found throughout the plot variation in SIF and this phenomenon change can be seen in Fig. 10(b). Whereas Fig. 10(c) shows the combination of adhesive thickness vs shear modulus has very small changes based on the contours. However, the fundamental studies explain that less adhesive thickness and actuator thickness will cause more reduction of SIF. Based on the existing work it has been recommended that the adhesive thickness 0.025 mm to 0.035 is more suitable for SIF reduction. Similarly, the actuator thickness of 0.5 mm has more reduction of SIF as compared to 1.0 mm and this can be seen well in contours.

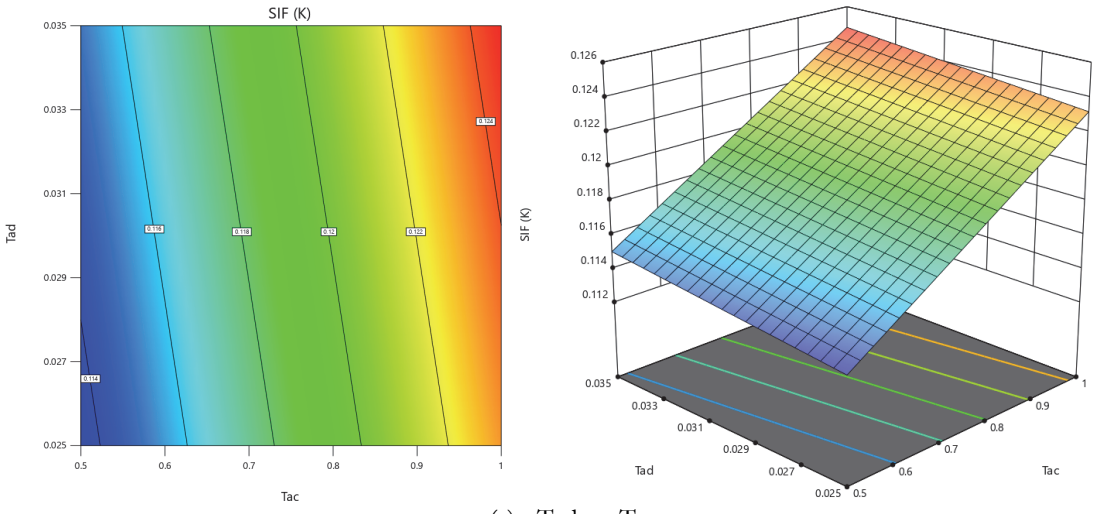

(a) Tad vs. Tac

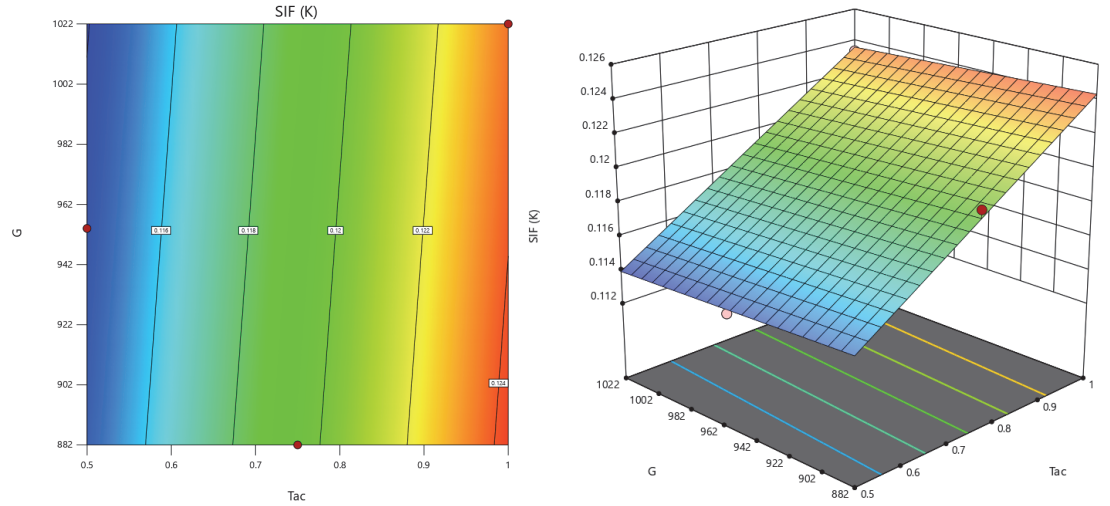

(b) G vs. Tac

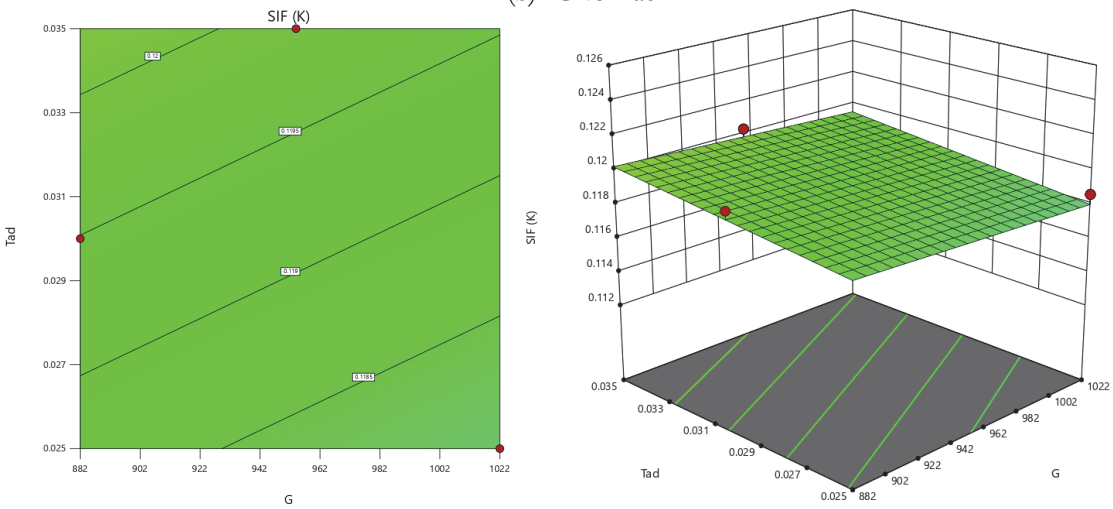

(c) Tad vs. G

Figure 10. Contours plot of SIF.

It was observed that in the response optimization table (Tab. 11), the value of SIF was as low as 0.102297 MPa √m. Nevertheless, the optimization should be moderated as other aspects of the patching process were also considered; the primary was out-plane bending and three-dimensional stress that are complicated and were developed by in-plane loading, although the shear stress in the adhesive or repaired structure surface need not be greater as it results in peeling. Thus, the value for SIF which is safer and justified must be around 0.112954 MPa √m as shown in Tab. 11. Therefore, to reduce SIF with a fitted value the parameters combination which can be considered are actuator thickness of 0.5 mm, adhesive thickness of 0.025 mm and shear modulus of 1022 MPa.

Variables	Settings	Value		Low limit	High limit	
Tac	Free			0.5	1.0	
G	Free			882	1022	
Tad	Free			0.025	0.035	
Response	Goal	Lower	Target	Upper	Weight	Importance
SIF (K)	Minimum	0.102297	0.113663	0.124878	1	1
Solution	Tac	G	Tad	SIF (K) Fit	Composite Desirability	
1	0.5	1022	0.025	0.112954	1	

Table 11. Response optimization: SIF (K) parameters

After optimizing the minimal reduction of SIF through the optimization method with a possible combination of parameters, the same parameters were applied to simulate the results. Finally, the obtained simulation results proved that the optimization method was useful in finding the optimal results. The optimum value of SIF obtained from the FE result was 0.11231 MPa √m which is close to the results obtained from the optimization approach shown in Tab. 11.

Conclusion

In the careful use of the design of experiments technique, the active repair of damaged structures using PZT actuators was thoroughly investigated in this work. The design of experiments approach shows the effectiveness was steadily established, providing a well-supported framework for the investigation. The comprehensive consideration of all significant characteristics and their complex relationships led to a thorough understanding of the underlying phenomena. Our attention was specifically on determining how different levels of shear modulus, adhesive thickness, and PZT actuator thicknesses reduce the stress intensity factor. This systematic study enabled us to identify the ideal PZT actuator design combinations, intending to lower stress intensity factor values. The importance of this work resides in its ability to advance the field of material optimization as well as enhance the structural integrity of damaged components. IN summary, our research demonstrated the relevance and efficiency of the DOE methodology in addition to introducing a novel way to structural rehabilitation. The results provide a foundation for improved PZT actuator designs with the potential to reduce stress intensity factors and increase the resilience of built structures.

Acknowledgement

This research was supported by the Ministry of Education of Malaysia (MOE) through Fundamental Research Grant Scheme (FRGS/1/2021/TK0/UIAM/01/5). Also, the authors acknowledge the support of the Structures and Materials (S&M) Research Lab of Prince Sultan University.

Conflicts of Interest

The authors declare no conflict of interest.

Availability of Data and Materials:

The datasets used during the current study are available from the corresponding author upon reasonable request.

References

[1] De Maio, U., Gaetano, D., Greco, F., Lonetti, P., Pranno, A. (2023). The damage effect on the dynamic characteristics of FRP-strengthened reinforced concrete structures, Compos. Struct., 309(January), pp. 116731, DOI: 10.1016/j.compstruct.2023.116731.

[2] Cha, Y.J., Buyukozturk, O. (2015). Structural damage detection using modal strain energy and hybrid multiobjective optimization, Comput. Civ. Infrastruct. Eng., 30(5), pp. 347–358, DOI: 10.1111/mice.12122.

[3] Wang, Q., Quek, S.T., Liew, K.M. (2002). On the repair of a cracked beam with a piezoelectric patch, Smart Mater. Struct., 11(3), pp. 404–410, DOI: 10.1088/0964-1726/11/3/311.

[4] Wang, Q., Quek, S.T. (2005). Repair of cracked column under axially compressive load via piezoelectric patch, Comput. Struct., 83(15–16), pp. 1355–1363, DOI: 10.1016/j.compstruc.2004.09.018.

[5] Rogers, C.A. (1993). Intelligent Material Systems — The Dawn of a New Materials Age, J. Intell. Mater. Syst. Struct.,

4(1), pp. 4–12, DOI: 10.1177/1045389X9300400102.
[6] Wang, Q., Duan, W.H., Quek, S.T. (2004). Repair of notched beam under dynamic load using piezoelectric patch, Int. J. Mech. Sci., 46(10), pp. 1517–1533, DOI: 10.1016/j.ijmecsci.2004.09.012.
[7] Shah, D.K., Joshi, S.P., Chan, W.S. (1994). Stress concentration reduction in a plate with a hole using piezoceramic layers, Smart Mater. Struct., 3(3), pp. 302–308.
[8] Alaimo, A., Milazzo, A., Orlando, C. (2011). On the dynamic behavior of piezoelectric active repair by the boundary element method, J. Intell. Mater. Syst. Struct., 22(18), pp. 2137–2146, DOI: 10.1177/1045389X11425281.
[9] Alaimo, A., Milazzo, A., Orlando, C. (2009). Boundary elements analysis of adhesively bonded piezoelectric active repair, Eng. Fract. Mech., 76(4), pp. 500–511, DOI: 10.1016/j.engfracmech.2008.10.008.
[10] Platz, R., Stapp, C., Hanselka, H. (2011). Statistical approach to evaluating reduction of active crack propagation in aluminum panels with piezoelectric actuator patches, Smart Mater. Struct., 20(8), pp. 085009, DOI: 10.1088/0964-1726/20/8/085009.
[11] Abuzaid, A., Hrairi, M., Dawood, M.S.I. (2015). Survey of Active Structural Control and Repair Using Piezoelectric Patches, Actuators, 4(2), pp. 77–98, DOI: 10.3390/act4020077.
[12] Abuzaid, A., Hrairi, M., Dawood, M.S. (2017). Modeling approach to evaluating reduction in stress intensity factor in center-cracked plate with piezoelectric actuator patches, J. Intell. Mater. Syst. Struct., 28(10), pp. 1334–1345, DOI: 10.1177/1045389X16672562.
[13] Abuzaid, A., Hrairi, M., Dawood, M.S. (2018). Experimental and numerical analysis of piezoelectric active repair of edge-cracked plate, J. Intell. Mater. Syst. Struct., 29(18), pp. 3656–3566, DOI: 10.1177/1045389X18798949.
[14] Abuzaid, A., Dawood, M.S., Hrairi, M. (2015). Effects of Adhesive Bond on Active Repair of Aluminium Plate Using Piezoelectric Patch, Appl. Mech. Mater., 799–800, pp. 788–793, DOI: 10.4028/www.scientific.net/AMM.799-800.788.
[15] Abuzaid, A., Shaik Dawood, M.S.I., Hrairi, M. (2015). The effect of piezoelectric actuation on stress distribution in aluminum plate with circular hole, ARPN J. Eng. Appl. Sci., 10(21), pp. 9723–9729.
[16] Aabid, A., Hrairi, M., Dawood, M.S.I.S. (2019). Modeling Different Repair Configurations of an Aluminum Plate with a Hole, Int. J. Recent Technol. Eng., 7(6S), pp. 235–240.
[17] Anjum, A., Aabid, A., Hrairi, M. (2023). Analysis of damage control of thin plate with piezoelectric actuators using finite element and machine learning approach, Frat. Ed Integrita Strutt., 66, pp. 112–126, DOI: 10.3221/IGF-ESIS.66.06.
[18] Aabid, A., Hrairi, M., Mohamed Ali, S.J., Ibrahim, Y.E. (2023). Review of Piezoelectric Actuator Applications in Damaged Structures: Challenges and Opportunities, ACS Omega, 8, pp. 2844–2860, DOI: 10.1021/acsomega.2c06573.
[19] Aabid, A., Parveez, B., Raheman, M.A., Ibrahim, Y.E., Anjum, A., Hrairi, M., Parveen, N., Zayan, J.M. (2021). A review of piezoelectric materials based structural control and health monitoring techniques for engineering structures : challenges and opportunities, Actuators, 10(5), pp. 101, DOI: 10.3390/ act10050101.
[20] Aabid, A., Raheman, A., Ibrahim, Y.E., Anjum, A., Hrairi, M., Parveez, B., Parveen, N., Zayan, J.M. (2021). A Systematic Review of Piezoelectric Materials and Energy Harvesters for Industrial Applications, Sensors, 21, pp. 1–28, DOI: 10.3390/s21124145.
[21] F. A. E. Crew, Edinburgh D. Ward Cutler, R. (1934). Statistical Methods for Research Workers, London.
[22] Montgomery, D.C. (2013). Design and Analysis of Experiments, John Wiley & Sons, Inc.
[23] Aabid, A., Hrairi, M., Ali, J.S.M. (2020). Optimization of composite patch repair for center-cracked rectangular plate using design of experiments method, Mater. Today Proc., 27(Part 2), pp. 1713–1719, DOI: 10.1016/j.matpr.2020.03.639.
[24] Aabid, A. (2023). Optimization of Reinforcing Patch Effects on Cracked Plates Using Analytical Modeling and Taguchi Design, Materials (Basel)., 16(12), pp. 4348.
[25] Aabid, A., Ibrahim, Y.E., Hrairi, M. (2023). Optimization of Structural Damage Repair with Single and Double-Sided Composite Patches through the Finite Element Analysis and Taguchi Method, Materials (Basel)., 16(4), pp. 1581.
[26] Aabid, A., Hrairi, M., Ali, J.S.M., Sebaey, T.A. (2022). A Review on Reductions in the Stress-Intensity Factor of Cracked Plates Using Bonded Composite Patches, Materials (Basel)., 15(3086), pp. 20.
[27] Aabid, A., Baig, M., Hrairi, M. (2023). Advanced Composite Materials for Structural Maintenance, Repair, and Control, Materials (Basel)., 16(2), pp. 1–3.
[28] Aabid, A., Hrairi, M., Abuzaid, A., Mohamed Ali, J.S. (2021). Estimation of stress intensity factor reduction for a center-cracked plate integrated with piezoelectric actuator and composite patch, Thin-Walled Struct., 158, DOI: 10.1016/j.tws.2020.107030.
[29] Aabid, A. (2020).Hybrid repair of cracked plates strengthened with composite patches and piezoelectric actuators. International Islamic University Malaysia.
[30] ANSYS Inc. (2017). ANSYS FLUENT 18.0: Theory Guidance, Canonsburg PA.

[31] Samaei, M., Zehsaz, M., Chakherlou, T.N. (2015). Experimental and numerical study of fatigue crack growth of Aluminum alloy 2024-T3 single lap simple bolted and hybrid (adhesive / bolted) joints, Eng. Fail. Anal. J., DOI: 10.1016/j.engfailanal.2015.10.013.
[32] Sun, G., Liu, X., Zheng, G., Gong, Z., Li, Q. (2018). On fracture characteristics of adhesive joints with dissimilar materials - An experimental study using digital image correlation (DIC) technique, Compos. Struct., DOI: 10.1016/j.compstruct.2018.06.018.
[33] Tada, H., Paris, P.C., Irwin, G.R. (2000). The Stress Analysis of Cracks Handbook, Third Edition, DOI: 10.1115/1.801535.
[34] Yala, A.A., Megueni, A. (2009). Optimisation of composite patches repairs with the design of experiments method, Mater. Des., 30, pp. 200–205, DOI: 10.1016/j.matdes.2008.04.049.
[35] Yala, A.A., Demouche, N., Beddek, S., Hamid, K. (2018). Full Analysis of All Composite Patch Repairing Design Parameters, Iran. J. Mater. Sci. Eng., 15(4), pp. 70–77, DOI: 10.22068/ijmse.15.4.70.
[36] Fekih, S.M., Albedah, A., Benyahia, F., Belhouari, M., Bouiadjra, B.B., Miloudi, A. (2012). Optimisation of the sizes of bonded composite repair in aircraft structures, Mater. Des., 41, pp. 171–176, DOI: 10.1016/j.matdes.2012.04.025.
[37] Richard, N.M. (2014). How To Use MINITAB: Design Of Experiment.
[38] Clements, R.B. (1991). Handbook of Statistical Methods in Manufacturing, Prentice Hall Direct.